Microdomains in Block Copolymers and Multiplets in Ionomers: Parallels in Behavior

Irina A. Nyrkova,*,† Alexei R. Khokhlov,*,† and Masao Doi

Department of Applied Physics, Nagoya University, Chikusa-ku, Nagoya 464, Japan

Received November 30, 1992; Revised Manuscript Received March 11, 1993

ABSTRACT: The microdomain structure in block-copolymer melts with short A blocks which strongly attract each other separated by long B blocks is studied for the case of narrow interphases between the microdomains. It is shown that as the temperature is lowered (or attraction of A blocks becomes more intensive), the behavior of the system changes qualitatively: instead of the usual strong segregation regime a new regime emerges which we define as the "superstrong segregation regime". In this regime A chains within the micelles become practically completely extended and steric restrictions on the chain conformations in the micelles become important. Although the superstrong segregation regime is not characteristic for ordinary block copolymers, it is easily realized for the case when one of the blocks is ionomeric. By considering the limiting case of one monomer link in the A block we obtain the results for microdomain (multiplet) structure in random ionomers. In most cases multiplets in ionomers correspond to microdomains in block copolymers in the superstrong segregation regime. We calculate the limiting size of the multiplet, the average distance between the multiplets, and the expansion of the chains in ionomer melts. The comparison of multiplets for random and telechelic ionomers is also performed.

1. Introduction

Recently, intensive attention has been paid to microphase separation in various polymer systems. Suppose that we have two immiscible polymer components A and B which for some reason cannot phase separate into macroscopic A-rich and B-rich phases. This conflict is resolved by the formation of microdomain structure (microphase separation) with alternating A-rich and B-rich domains of relatively small size which is controlled by the connectivity condition between the A and B components.

For a long time the only polymer systems for which the phenomenon of microphase separation was studied in detail were the melts and solutions of block copolymers with immiscible blocks. For this case, due to the fact that the blocks are linked into one chain by valency chemical bonds, the microdomain structure is formed instead of separation into macroscopic phases.[1-3] The morphology of this structure depends on the chain architecture and the relative length of the blocks. For example, for a diblock A–B copolymer with the number of monomer links in the blocks N_A and N_B, lamellar, cylindrical, or spherical microdomains can emerge.[1-5] For the case when the length of the A block is much smaller than that of the B block ($N_A \ll N_B$) the equilibrium microstructure corresponds to the spherical A-rich domains surrounded by the "sea" of B-rich regions (Figure 1). This case will be of special interest for the present paper. It should be noted that main theoretical and experimental work on the microdomain structures in block copolymers deals with diblocks, while much less attention was paid to the triblocks, polyblocks, and block-copolymer chains with more complicated architectures.[6-8]

Recently, it has been discovered that block copolymers are not unique in forming microdomain polymer structures. Among the examples are interpenetrating polymer networks[9,10] (here the connection between the interpenetrating A and B networks is ensured by the topological entanglements of A and B chains), weakly charged polyelectrolytes in poor solvents and mixtures of weakly charged polyelectrolytes[11-14] (for this case the role of the connection between different components is effectively played by the condition of total electroneutrality), and random copolymers, where microdomain structures are due to the fluctuations in local chemical composition (i.e. primary structure of the chain).[15-17] Thus, the concept of microphase separation has a much wider application in polymer physics than it was previously thought.

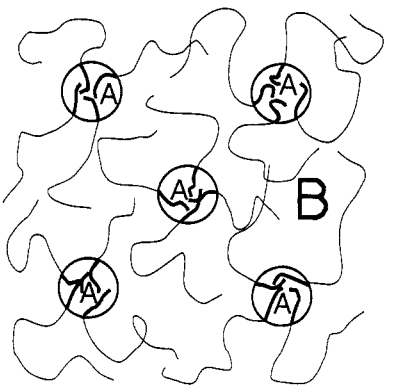

Figure 1. Spherical micelles in a diblock-copolymer melt ($N_A \ll N_B$), strong segregation regime.

There is one more class of polymer systems where microdomain structures have been known (under another name) and studied intensively for a long time. This is ionomers, which are ion-containing polymers in the medium of low polarity where practically all the counterions are not dissociated and form ion pairs with the ions of the polymer chains (free counterions are absent). Usually, ionomers are copolymers with a small fraction of A links carrying ion pairs incorporated into neutral B chains (Figure 2a). In the solutions or melts of ionomers due to the strong attraction between A dipoles they are associating to form what is called a multiplet structure (Figure 2b).[18] This structure was extensively studied both experimentally and theoretically.[18-21]

If we now switch to a block-copolymer language and describe the situation shown in Figure 2, we should say that we have some A–B copolymer with a few percent of A links which strongly attract each other and passive B links. Since the number of A links is much smaller, we may expect these links to be organized into small spherical

† Permanent address: Physics Department, Moscow State University, Moscow 117234, Russia.

0024-9297/93/2226-3601$04.00/0

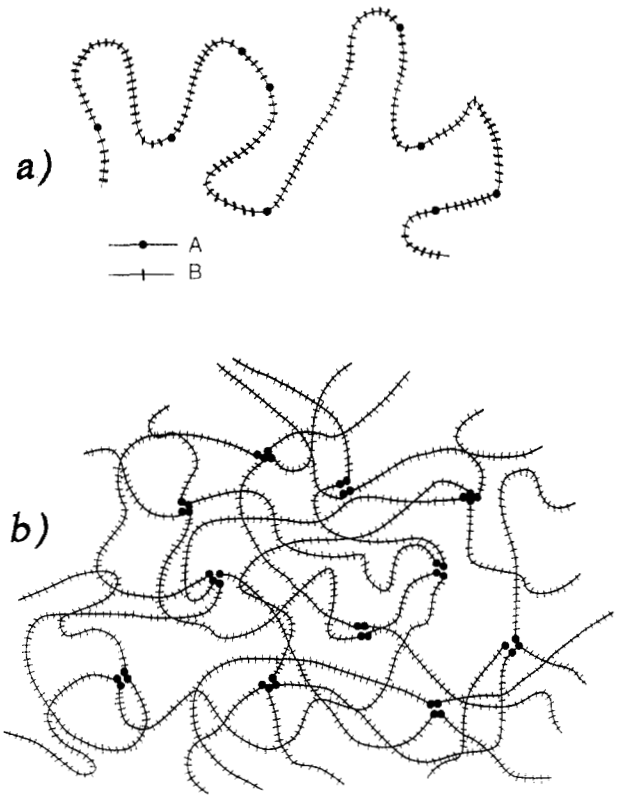

Figure 2. Chain of a random ionomer (a). Multiplet structure in the ionomer melt (b).

micelles (cf. Figure 1). It is clear that these micelles are just multiplets in the ionomer language. The main difference between Figures 1 and 2 is in the fact that for Figure 2 the number of A links in one A "block" is equal to one, thus the situation of Figure 2b should emerge as some limiting case ($N_A = 1$) of the microdomain structure of a block copolymer melt.

Another difference between Figures 1 and 2 is that the microdomain structure of Figure 1 is formed by diblock copolymers, so that one macromolecule visits only one spherical A micelle. The situation in Figure 2 corresponds to the limiting case $N_A = 1$ of the structure formed by polyblock macromolecules (Figure 3a) where the blocks of N_A A links are separated by long passive chains of N_B B links.

For the ionomer case the system similar to block copolymers with a small number of blocks can be found as well. This is the melt of telechelic ionomers, i.e. of molecules including a long neutral chain with ionomer links at both ends of this chain.[22-24] The microstructure formed by such molecules corresponds to the microstructure of a triblock A–B–A block copolymer (Figure 3b) in the limit when the number of links in the A blocks is equal to one.

Although the similarity between block-copolymer and ionomer behavior has been mentioned in several papers (see e.g. refs 22 and 25), the consequences which follow from this similarity were not explored in detail. It is the aim of the present paper to perform the quantitative comparison of the microstructures in block-copolymer and ionomer systems. Since the microdomain structures in block copolymers have been studied theoretically in a much more detailed manner than multiplets in ionomers, we will be able to extract from this comparison useful information for the structure of ionomer melts.

Simultaneously, comparison with ionomers will allow us to enrich the picture of possible regimes for block-

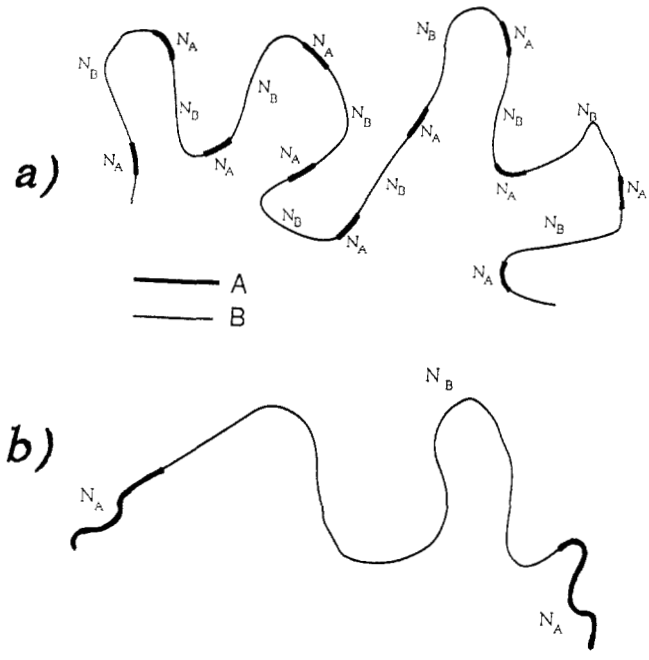

Figure 3. (a) Polyblock AB copolymer. (b) Triblock copolymer ABA.

copolymer spherical micelles (Figure 1). In addition to the weak segregation[4,26,27] and strong segregation[5,28,29] regimes for microdomain structure in block-copolymer melts we will define a superstrong segregation regime which happens when there is an extremely high attraction of the monomer links of one of the blocks. As a practical realization of this regime we have in mind, primarily, block copolymers with ionomeric and neutral blocks;[25] however any other systems with strongly attracting A blocks should show this behavior.

We will see that in most cases multiplets in ionomers correspond to microdomains in block copolymers in the superstrong segregation regime.

It was already mentioned that the system which is analogous to ordinary ionomers is a melt of polyblock copolymers (Figure 3a); telechelic ionomers correspond to triblocks (Figure 3b). Therefore, in the next section we will begin with the analysis of microdomain structures formed by block copolymers shown in Figure 3a or 3b, in the strong segregation regime. In section 3 we will define the superstrong segregation regime and discuss its relevance to microdomain structure in block copolymers with ionomeric blocks. Finally, in section 4 the consequences of the obtained results for ordinary ionomer melts will be described.

2. Microdomains in Block-Copolymer Melts. Strong Segregation Regime

Let us consider the microdomain structure formed by block copolymers including A blocks (number of monomer links N_A), which strongly attract each other, and B blocks (number of monomer links N_B). More precisely, we will consider regular polyblock copolymers with alternating A and B sections (Figure 3a) and triblock copolymers (Figure 3b). We will assume that $N_A \ll N_B$, and therefore A blocks form spherical micelles if the attraction between these blocks is strong enough.[5]

There are two main theoretical methods of describing microdomain structures in the block-copolymer melts: expansion of the free energy in the powers of local deviations in the concentration of A links from the average concentration ("weak segregation limit" which is valid near the critical point of microphase separation[4,26,27]) and self-

consistent calculation of the concentration profile of well-separated A and B domains with narrow interphases between them ("strong segregation limit"[5,28,29]). Since we have in mind further application to the case of ionomers where the attraction between A links is due to the dipole–dipole interaction and the corresponding characteristic energy can be much larger than kT,[30] we will confine ourselves to the consideration of domains with narrow interphases, i.e. to the strong segregation case.

The first question to be answered is the following: are all A blocks incorporated in the micelles or are there "free" A blocks within the B-rich domains? In Appendix 1 it is shown that, in the strong segregation limit, if the micelles are formed, the number of such free A blocks is exponentially small; therefore in the subsequent consideration we will assume that all A blocks belong to micelles.

This fact allows us to estimate the average distance between neighboring micelles, λ, from the simple space-filling arguments. Indeed, on the one hand, the average volume per micelle is $\sim\lambda^3$. On the other hand, this volume can be estimated as

$$Q(v_A N_A + v_B N_B) \quad \text{for polyblocks}$$

$$Q(v_A N_A + {}^1/_2 v_B N_B) \quad \text{for triblocks}$$

where Q is the average number of A blocks in the micelle and v_A and v_B are the volumes of A and B links; the values of v_A and v_B are connected with the densities, ρ_A and ρ_B, of the bulk A and B chains by the relations $v_A = \mu_A/\rho_A\mathcal{N}$ and $v_B = \mu_B/\rho_B\mathcal{N}$, where μ_A and μ_B are the molar masses of A and B monomer links and $\mathcal{N}$ is the Avogadro number. Thus

$$\lambda \equiv [\gamma Q(v_A N_A + \varkappa v_B N_B)]^{1/3} \tag{1}$$

where

$$\varkappa = 1 \quad \text{for polyblocks} \tag{2}$$

$$\varkappa = {}^1/_2 \quad \text{for triblocks}$$

The coefficient γ which is of the order unity depends on the type of spatial arrangement of the spherical micelles. For example, for body-centered cubic lattice, which is usually considered as the most favorable in the strong segregation limit, $\gamma = 2$, provided that λ is the main lattice site length. For the case $N_B \gg N_A$ under consideration in the present paper we finally obtain the following expression for the average intermicellar distance:

$$\lambda = (\gamma Q \varkappa v_B N_B)^{1/3} \tag{3}$$

As will be shown later, the value of Q is independent of N_B; therefore λ is proportional to $N_B{}^{1/3}$. This shows from the very beginning that the average intermicellar distance varies with the increase of N_B more slowly than the Gaussian dimension of the B coil (which is proportional to $N_B{}^{1/2}$).

To estimate the average number of A blocks in the micelle, Q, and the radius of the micelle, R, let us consider the free energy of the system of micelles (cf. refs 5, 31–33). It can be written as a sum of three terms:

$$F = F_1 + F_2 + F_3 \tag{4}$$

where F_1 is the free energy of micellar interfaces and F_2 and F_3 correspond to the conformational entropy of expansion of B and A chains (the fact of significant expansion of A chains in spherical micelles and B chains in the region close to A micelles in the strong segregation limit was proven in ref 5).

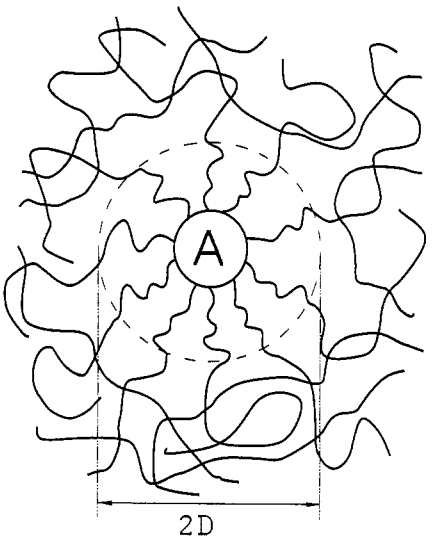

Figure 4. Structure of the spherical A micelle in the strong segregation regime. B chains are strongly extended within the sphere of radius D. "Foreign" B chains do not penetrate inside this region.

It is easy to understand that the interfacial free energy F_1 has the form

$$F_1 = 4\pi R^2 \delta \mathbf{N}/Q \tag{5}$$

where $\mathbf{N}$ is the total number of A blocks in the system (thus the number of micelles is $\mathbf{N}/Q$) and δ is the surface tension coefficient. It is the value of δ that will determine in our theory the degree of immiscibility of A and B blocks.

To write down the expression for F_2, it should be noted that B blocks are extended mainly in the regions neighboring A micelles (Figure 4). The degree of this extension can be estimated from the following considerations (cf. ref 5). Let us assume that the average spatial position of B links separated by n links from the A–B junction point (which lies in the interfacial region) corresponds to the distance $r(n)$ from the center of the micelle. It is natural to assume (and this is confirmed by the exact calculation; see below and ref 5) that inside some sphere of radius D centered at the center of the micelle ($D \gg R$, Figure 4) the A chains entering a given micelle dominate over the "foreign" A chains. Therefore, at $r < D$ from the space-filling arguments we obtain

$$\frac{4\pi}{3} r^3(n) = \frac{4\pi}{3} R^3 + 2\varkappa Q v_B n \tag{6}$$

The factor $\varkappa$ (see eq 2) appears here because for polyblocks the number of B chains emanating from the micelle is twice as large as the number of A chains in the micelle. By generalizing the formula $F_{elastic} \cong kT(3R^2/2Nal)$ (where T is the temperature and k is the Boltzmann constant) for the case of inhomogeneous expansion, we obtain

$$dF_{elastic} = 3kT[r(n + dn) - r(n)]^2/2la\,dn = \frac{3}{2}kT\left(\frac{dr}{dn}\right)^2 \frac{dn}{la} \tag{7}$$

If the dependence $r(n)$ for B links is given by eq 6, the free energy of expansion of B chains can be written in the form

$$F_2 = 2\varkappa \mathbf{N} \frac{3}{2} kT \int_0^{n_{max}} \left(\frac{dr}{dn}\right)^2 \frac{dn}{l_B a_B} = \frac{3\varkappa^2}{2\pi} \frac{kT}{R} \frac{v_B}{l_B a_B} \mathbf{N} Q \tag{8}$$

where a_B and l_B are the monomer link length (i.e. the contour length of the chain per one monomer link) and

the Kuhn segment length of the B chains, correspondingly. In eq 8 we have taken into account that the number of extended sections of B chains is 2N for polyblocks and N for triblocks. Thus, the upper limit of the integration in eq 8 is unessential and it turns out that the major part of the free energy F_2 is concentrated near the micelle (at the distances of order $r \ll D$).

The scaling form for F_3 is easily established (cf. ref 34):

$$F_3 \sim kT\mathbf{N}R^2/N_A a_A l_A$$

where a_A and l_A are the contour chain length per one monomer link and the Kuhn segment length of the A chains, correspondingly. The numerical coefficient in this formula for the case of a spherical micelle can be derived by applying the method of ref 5. In Appendix 2 it is shown that this coefficient is equal to $3\pi^2/20$ for polyblocks and $3\pi^2/80$ for triblocks. Using the notation (2) introduced previously, we can write finally

$$F_3 = \frac{3\pi^2}{20}\varkappa^2 kT\mathbf{N}\frac{R^2}{N_A a_A l_A} \tag{9}$$

The value of the radius of the micelle, R, in the expressions (5), (8), and (9) is directly connected to Q due to the space-filling condition (cf. eq 6):

$$R = \left[\frac{3}{4\pi}Qv_A N_A\right]^{1/3} \tag{10}$$

Equations 5 and 8–10 define completely the free energy (4). The chemical structure of A and B chains enters through the parameters a_A, l_A, v_A; a_B, l_B, v_B. To simplify the notation in the formulas below it is convenient to introduce the cross section, s_A and s_B, of A and B chains and also the total contour lengths, L_A and L_B, of the blocks:

$$s_A = v_A/a_A = \mu_A/a_A\rho_A\mathcal{N},$$
$$s_B = v_B/a_B = \mu_B/a_B\rho_B\mathcal{N}, L_A = a_A N_A, \quad L_B = a_B N_B \tag{11}$$

In this notation the free energy (4) takes the form independent of the parameters a_A and a_B:

$$F = \mathbf{N}kT\left(\frac{36\pi}{s_A L_A}\right)^{1/3}\left[\frac{\delta}{kT}\frac{s_A L_A}{Q^{1/3}} + \frac{\varkappa^2}{2\pi}Q^{2/3}\frac{s_B}{l_B}\theta\right] \tag{12}$$

where we have defined

$$\theta \equiv 1 + \frac{3\pi^2}{40}\frac{s_A l_B}{s_B l_A} \tag{13}$$

It should be noted that the free energies of extension of B and A chains, F_2 and F_3, show the same dependence on Q and $\mathbf{N}$; if $s_A \sim s_B$ and $l_A \sim l_B$, these contributions to the free energy are of the same order of magnitude.

The minimization of the free energy (12) with respect to Q gives the equilibrium value for the number of A blocks in the micelle

$$Q = \frac{\pi}{\varkappa^2}\frac{\delta}{kT}\frac{s_A L_A l_B}{s_B\theta} \tag{14}$$

thus, from eq 10 we have

$$R = \left[\frac{3}{4\varkappa^2}\frac{\delta}{kT}\frac{s_A{}^2 L_A{}^2 l_B}{\theta s_B}\right]^{1/3} \tag{15}$$

Combining the result (14) with eq 3 we obtain the following expression for the intermicellar spacing λ:

$$\lambda = \left[\frac{\pi\gamma}{\varkappa}\frac{\delta}{kT}\frac{L_B l_B L_A s_A}{\theta}\right]^{1/3} \tag{16}$$

Equations 14–16 give main equilibrium characteristics of the system of spherical micelles in the strong segregation limit. To complete the evaluation of the structure of the micelles, let us also estimate the characteristic radius D of the sphere around the micelle within which the number of foreign B chains (i.e. B chains which are not directly connected to a given micelle) is negligible (Figure 4). This will allow us to justify the inequality $D \gg R$ which was used in deriving the expression (8) for the free energy F_2.

It is clear that when the fraction of foreign chains becomes significant, the Edwards mechanism of screening of correlations in concentrated systems comes into play;[35] therefore the chain stretching should vanish. Thus, at $r \sim D$ the local expansion of the B chains should be of order unity, i.e.

$$\left.\frac{dr}{dn}\right|_{\text{from (6)}} \sim \left.\frac{dr}{dn}\right|_{\text{for Gaussian chain}} \quad \text{at } r \sim D$$

This gives the estimate

$$D \sim \varkappa Q\frac{s_B}{l_B} \sim \frac{1}{\varkappa}\frac{\delta}{kT}\frac{s_A L_A}{\theta} \tag{17}$$

where we have used eq 14.

By comparing eqs 15 and 17, we obtain $R \ll D$ at

$$\frac{\delta}{kT} \gg \theta\sqrt{\frac{\varkappa l_B}{s_A s_B L_A}} \tag{18}$$

In Appendix 1 it is shown that the condition (18) is always valid if the free energy of micelle formation is negative, i.e. if the micelles are formed in the equilibrium. Therefore the inequality $R \ll D$ is justified independently of the chain characteristics of A and B blocks.

It was already noted above that since $\lambda \sim L_B{}^{1/3}$ and the average Gaussian dimension of a B coil is proportional to $L_B{}^{1/2}$, at large enough values of L_B the B chains should connect rather remote micelles, and not the micelles which are neighboring each other. Now we can study the interrelation between λ and the average size of B chains quantitatively. From eq 16 it follows that if

$$\frac{\delta}{kT} \ll \left(\frac{\delta}{kT}\right)_{cr} \equiv \frac{\varkappa\theta(L_B l_B)^{1/2}}{L_A s_A} \tag{19}$$

the intermicellar distance λ is much smaller than the Gaussian dimension of the B chain $(L_B l_B)^{1/2}$. Thus, for small enough values of the parameter δ/kT, i.e. for high enough temperatures [but these temperatures are low enough to ensure a strong segregation limit (cf. inequality (14))], B chains indeed connect remote micelles, which means that in the middle of the B-rich region foreign chains dominate over the chains going to the closest micelles. This fact indicates also that for the major part of a B chain the statistics is Gaussian; thus for the end-to-end distance of these chains we can write $R_B \cong (L_B l_B)^{1/2}$.

On the other hand, if $\delta/kT \gg (\delta/kT)_{cr}$ the radius of the micelles (and simultaneously the value of Q) becomes so large that inequality $\lambda \ll R_B$ is no longer fulfilled. Since λ cannot be larger than R_B, we come to the conclusion that in this regime $\lambda \sim R_B$ and $R_B \gg (L_B l_B)^{1/2}$; i.e. the B chains are strongly extended. In full accord with this estimation it turns out that when the inequality (19) ceases to be fulfilled, the value of D becomes of order of λ (cf. eqs 16 and 17).

Thus, we are coming to the following picture of possible regimes in the strong segregation limit. According to ref 5 in the highly assymmetric case $N_A \ll N_B$ under consideration micelles begin to form at some value of $\delta/kT = (\delta/kT)_0$ and from the very beginning the interphases are narrow; i.e. we are in the strong segregation regime. With

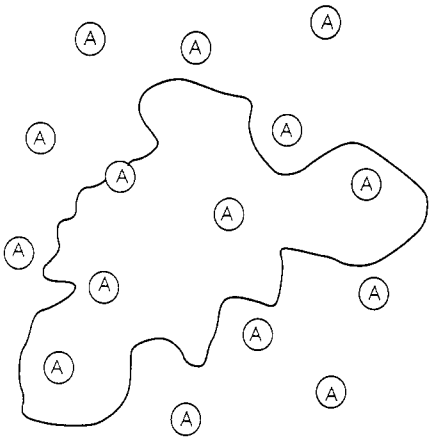

Figure 5. B block making loop return to the initial micelle.

a further increase of δ/kT, two regimes become possible.

(a) $(\delta/kT)_0 \lesssim \delta/kT \ll (\delta/kT)_{cr}$. Here the micelles are surrounded by the regions of thickness D ($R \ll D \ll \lambda \ll R_B$) where the B chains are stretched. B chains connect relatively remove micelles; therefore the probability β of chain return with loop formation (Figure 5) is rather low: $\beta \sim \lambda^3/R_B^3 \ll 1$.

(b) $\delta/kT \gg (\delta/kT)_{cr}$. Here the micelles are so large that all three length parameters, λ, D, and R_B, are of the same order of magnitude. The B chains connect mainly neighboring micelles and are strongly extended. Therefore the loop probability parameter introduced above is of order unity, $\beta \sim \lambda^3/R_B^3 \sim 1$.

3. Microdomains in Block-Copolymer Melts. Superstrong Segregation Regime

We can see that the average dimension of the micelles increases continuously with the decrease of temperature. Equations 14 and 15 predict even infinite increase, as $T \to 0$ ($\delta \to +\infty$). It is clear, however, that there are natural limits for such an increase. There are two main physical reasons for this.

(i) With the increase in R, the value of R may exceed the dimension of the fully stretched A chain $L_A = N_A a_A$; this is, of course, impossible.

(ii) With the increase in Q, it may turn out that all the surface of the micelle is totally occupied by A–B junction points, and there is no place on the surface to incorporate one more A chain to the micelle.

The restrictions i and ii impose limits to the increase of the micellar size with the decrease of temperature. When we reach one of these limits, we come to a qualitatively new regime of micellar structure. We will call this regime a "superstrong segregation regime". Up to now it has not attracted much attention, because it is not very realistic for usual block copolymers. However, we will show below that for ordinary ionomers and also for block copolymers with one ionomeric and one neutral block this regime can be easily achieved and, in many cases, is the most characteristic.

First of all, let us estimate the temperatures at which the restrictions i and ii become important.

From eq 11 it follows that the inequality $2\varkappa R \lesssim L_A$ does not hold if

$$\frac{\delta}{kT} \gtrsim \frac{\theta}{6\varkappa}\frac{L_A s_B}{s_A^2 l_B} \tag{20}$$

Here we have used again the notation (2) and have taken into account that for triblocks the free ends of some A blocks should reach the center of the micelle and for polyblocks some A blocks should visit the center having the ends at the surface of the spherical micelle.

On the other hand, if we introduce a surface area, s_{AB}, per one A–B junction point, the condition $4\pi R^2 \gtrsim 2\varkappa Q s_{AB}$ associated with restriction ii ceases to be fulfilled at (there are two A–B junction points per each A block in polyblocks and one in triblocks)

$$\frac{\delta}{kT} \gtrsim \frac{9\theta}{2\varkappa}\frac{s_A s_B L_A}{s_{AB}^3 l_B} \tag{21}$$

(to derive eq 21 we used expressions 14 and 15 of the strong segregation limit).

The expressions in the right-hand sides of the inequalities (20) and (21) are similar: they depend on L_A, s_B, l_B, and θ in the same way and they differ by the factor $27 s_A^3/s_{AB}^3$. Therefore for the most common case when the cross-sections of A chains and A–B junctions are close to each other, $s_A \approx s_{AB}$, the limiting factor is restriction i, i.e. the stretching of A chains, and the region of existence of the superstrong segregation regime is defined by the inequality (20). On the other hand, if B chains are bulky, the value of s_{AB} can be much larger than s_A. In this case the superstrong segregation regime is defined by the inequality (21).

In the general case it is the smallest of the right-hand sides of inequalities (20) and (21) that is important. In further consideration in order to simplify the formulas we will introduce the notation

$$\Omega \equiv \min\{1; 3s_A/s_{AB}\} \tag{22}$$

Then the conditions (20) and (21) defining the superstrong segregation regime can be incorporated into one inequality

$$\frac{\delta}{kT} \gtrsim \left(\frac{\delta}{kT}\right)_{SS} \equiv \frac{\theta}{6\varkappa}\Omega^3\frac{L_A s_B}{l_B s_A^2} \tag{23}$$

The value of $(\delta/kT)_{SS}$ in eq 23 corresponds to the crossover transition from the strong to the superstrong segregation regime.

In the superstrong segregation regime the values of Q and R no longer increase with the decrease of temperature. These are constant micellar characteristics which depend on the length of the A blocks, L_A, and on the parameters of the A and B chains. Let us denote these characteristics as Q_{SS} and R_{SS}. Although the exact values of Q_{SS} and R_{SS} cannot be derived from the simple theory outlined above, it is natural to assume that if we substitute into eqs 14 and 15 the crossover value $(\delta/kT)_{SS}$ (eq 23) we obtain reasonably accurate expressions for Q_{SS} and R_{SS}. This procedure gives

$$Q_{SS} = \frac{\pi}{6\varkappa^3}\Omega^3\frac{L_A^2}{s_A} \tag{24}$$

$$R_{SS} = \frac{L_A}{2\varkappa}\Omega \tag{25}$$

The intermicellar spacing λ_{SS} and the diameter D_{SS} of the region of the extended B chains (cf. the derivation of eq 17) in the superstrong segregation regime are given by

$$\lambda_{SS} = \Omega\left[\frac{\gamma\pi}{6\varkappa^2}\frac{s_B}{s_A}L_A^2 L_B\right]^{1/3} \tag{26}$$

$$D_{SS} = \frac{\Omega^3}{6\varkappa^2}\frac{L_A^2 s_B}{l_B s_A} \tag{27}$$

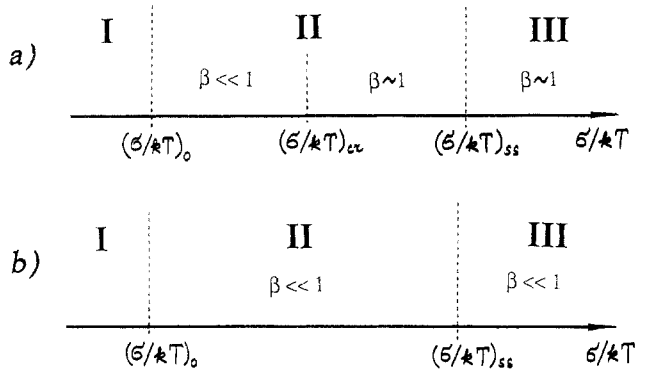

Figure 6. Possible regimes of behavior of a block-copolymer melt with $N_A \ll N_B$ depending on the value δ/kT: (I) homogeneous melt, (II) strong segregation regime, (III) superstrong segregation regime. $(\delta/kT)_0$ corresponds to the threshold of micelle formation. (a) $(\delta/kT)_{cr} < (\delta/kT)_{SS}$ and (b) $(\delta/kt)_{cr} > (\delta/kt)_{SS}$. The loop formation probability, β, is indicated for each of the regimes.

We have seen above that in the strong segregation limit the important difference in the microdomain structure comes from the fact whether λ is much smaller than the average size of the B chains, R_B ($\lambda \ll R_B$), or λ is of the order R_B ($\lambda \sim R_B$). It was shown that at $\delta/kT \gg (\delta/kT)_{cr}$ $\lambda \sim R_B$, while at $\delta/kT \ll (\delta/\mathrm{kT})_{cr}$ $\lambda \ll R_B$. By comparing the crossover value $(\delta/kT)_{cr}$ (eq 19) with the boundary of superstrong segregation regime $(\delta/kT)_{SS}$ (eq 23), we can see that if

$$(\delta/kT)_{cr} < (\delta/kT)_{SS} \quad \text{or} \quad L_A > \varkappa (L_B l_B^3)^{1/4} \left(\frac{s_A}{s_B \Omega^3}\right)^{1/2} \tag{28}$$

the value of $(\delta/kT)_{cr}$ corresponds to the strong segregation regime. This means that while the temperature is lowered, both cases $\lambda \ll R_B$ and $\lambda \sim R_B$ are realized within this regime before we reach the superstrong segregation behavior. Another possibility is that $(\delta/kT)_{cr}$ lies within the superstrong segregation regime (this happens if the inequality opposite to (28) is valid); then only the case $\lambda \ll R_B$ can be realized in the strong segregation region, and when the temperature is lowered we are entering the superstrong segregation regime before λ becomes of order R_B.

The possible regimes of the behavior of the system under consideration are summarized in Figure 6. Figure 6a corresponds to the case $(\delta/kT)_{cr} < (\delta/kT)_{SS}$, and Figure 6b, to the opposite inequality. The loop formation probability β ($\beta \sim \lambda^3/R_B^3$, see Figure 5) in the superstrong segregation regime is of order unity for the case of Figure 6a (when the inequality (28) is valid) and much less than unity for Figure 6b.

Equation 23 indicates that it is rather difficult to observe the superstrong segregation regime for conventional block copolymers: there is a large factor L_A in the right-hand side of eq 23. This is the reason why this regime has not been discussed in the literature up to now. This regime can be reached only if (i) there is a very strong attraction between A blocks and (ii) the length of A blocks is relatively small. However, although ordinary block copolymers do not fulfill these requirements, block copolymers with relatively short ionomeric blocks of the type studied in ref 25 are just good objects to observe a superstrong segregation regime.

Indeed, the characteristics of the microdomain structures observed in ref 25 are very similar to what can be expected for the superstrong segregation regime. The value of the micelle radius R was shown to be a linear function of L_A (cf. eq 25) instead of dependent on $L_A^{2/3}$ for the strong segregation regime. The observed radius of the micelles corresponded to very strongly extended chains. The intermicellar distance was found to be in some cases lower than the Gaussian radius of the B chains. The number of B chains per micelle ($2Q$ in our notation) was much higher than is observed for normal block copolymers. Finally, the contact micelle surface area per A chain was found to be remarkably constant for all the block copolymers studied (with diverse values L_A and L_B). All these results clearly show that the micelles which were observed in ref 25 correspond to the superstrong segregation regime.

4. Microdomains (Multiplets) in Ionomer Melts

4.1. Extrapolation Formula for Multiplet Size. Another example of the system where the superstrong segregation regime plays an important role is ordinary ionomers (Figure 2). It was already noted in the Introduction that this case corresponds to the limit $N_A = 1$ (or $L_A = a_A$). But in this case the values $\delta/kT > (\delta/kT)_{SS}$ (eq 23) are easily accessible; in fact, if all the microscopic length scales in the system are of the same order of magnitude ($l_A \sim l_B \sim a_A \sim a$; $s_A \sim s_B \sim a^2$), eq 23 for $L_A = a_A$ corresponds to $\delta a^2/kT > 1$ and thus for strongly attracting A links it is always fulfilled. Therefore, it is the superstrong segregation regime that should be most suitable to describe the multiplet structure in ordinary random ionomers. Let us now analyze the consequences which follow from this statement.

By assuming that $L_A = a_A$ in eqs 24 and 25, it is possible to obtain the following values for the number of the dipoles in the ionomer multiplet, $(Q_{SS})_I$, and the radius of the multiplet, $(R_{SS})_I$:

$$(Q_{SS})_I = \frac{\pi \Omega^3 a_A^2}{6\varkappa^3 s_A} = \frac{\pi \Omega^3 a_A^3 \rho_A}{6\varkappa^3 \mu_A} \mathcal{N} \tag{29}$$

$$(R_{SS})_I = \frac{\Omega}{2\varkappa} a_A \tag{30}$$

where the second expression for $(Q_{SS})_I$ in eq 29 is written in this form by using eq 11.

Of course, this procedure is not exact. Equations 29 and 30 are based on the long-chain statistics of A chains in the micelles (cf. eq 9); thus they cannot be accurate for $N_A = 1$. However, it seems to us natural to assume continuity of properties when passing from the limit $N_A \gg 1$ to $N_A = 1$ and to examine its outcome.

This approach can be justified by the fact that even if F_3 (the elastic free energy of A blocks) is put to zero, which is another limiting case, the free energy expression (12) remains essentially unchanged because the contributions of F_2 and F_3 are similar.

Therefore, we will use all the formulas derived above to analyze also the random ionomer case $L_A = a_A$. The only problem which needs clarification is what we should take as a value of a_A in eqs 29 and 30. For the case of block copolymers a_A has the exact meaning: contribution of one ionomer link to the contour length of the chain. However, it is clear that for the case of random ionomers this contribution has little to do with the real geometry of the multiplet and with the restrictions i and ii which limit the maximum multiplet size. By reconsidering the derivation of the inequalities (20) and (21) which define the region of existence of the superstrong segregation regime, it is possible to conclude that for the case of lone ion pairs a_A should be taken as the distance between two ion pairs in the neighbor links in the chain consisting of only A links. We will assume this in the further consideration; we feel

that more detailed speculations on the value of a_A should depend on the exact chemical structure of the groups forming multiplets and are beyond the accuracy of the present theory. Most of the qualitative results and trends which are discussed below are independent of the exact value of the parameter a_A.

From eq 29 (see also eq 22), one can see that the number of dipoles in the multiplets, $(Q_{SS})_I$, depends on the geometry of an ionomeric link and its connection to the B chain, i.e. on s_{AB}. It is determined by the two types of geometrical restrictions which have the origin analogous to the points i and ii formulated in the beginning of section 3. The importance of the steric constraint of type ii for the calculation of the average number of dipoles in the multiplet was noted by Eisenberg in ref 18.

For many cases, however, it is restriction i which is the limiting factor for the growth of the multiplet size, since s_{AB} and s_A are usually close to each other. In this situation we obtain

$$(Q_{SS})_I = \frac{\pi a_A^2}{6\varkappa^3 s_A} = \frac{\pi a_A^3 \rho_A}{6\varkappa^3 \mu_A}\mathcal{N} \quad \text{and} \quad (R_{SS})_I = \frac{a_A}{2\varkappa} \tag{31}$$

where for telechelic ionomers $\varkappa = 1/2$ and for ordinary random ionomers $\varkappa = 1$ since, as it was noted in the Introduction, the former situation is a limiting case of triblock copolymers, while the latter situation corresponds to the limit $N_A = 1$ of polyblock copolymers.[36a]

For the multiplets formed by sulfonated polystyrene links, if we take a_A as the distance between two ion pairs in the neighbor links along the fully sulfonated chain, we have $a_A = 13$ Å. For $\rho_A = 1.8$ g/cm^3 and $\varkappa = 1$, we get $(Q_{SS})_I = 5.6$ which is rather close to experimental observations[18] for random sulfonated polystyrene ionomers. The agreement may be fortuitous, since the exact number for $(Q_{SS})_I$ or $(R_{SS})_I$ depends essentially on the definition of the parameter a_A which is not unambigous.

Returning to the problem of the role of restrictions i and ii for ionomers, it should be noted that restriction i is not always the dominant one. For example, for ionomers with bulky B chains (large values of s_{AB}) restriction ii is more important. This restriction leads to lower values of $(Q_{SS})_I$ for bulky B chains, as was observed experimentally.[22]

On the other hand, eq 29 indicates that the average number of dipoles in the multiplet for telechelics is 8 times larger than that for random ionomers. This result is independent of the details of the geometry of the chain and is considered to be valid generally.

Experimental comparative studies of random and telechelic ionomers were performed in refs 22–24. The general conclusion that the size of the multiplet for telechelics is much larger than for random ionomers agrees well with experimental observations. The ratio of the values of $(Q_{SS})_I$ for these two cases was reported to be from 3 to 10, which agrees reasonably well with the result obtained above (ionomer groups in random ionomers and telechelics, even being of the same chemical origin, cannot be completely identical).

The smooth crossover between telechelic and random ionomers was studied in ref 37 where the microstructure of ionomer melts with variable-length side chains was considered (ionomeric groups were at the ends of the side chains). Here short side chains are close to random ionomers, while long side chains correspond to telechelics. On the other hand, the geometry of ionomeric groups is the same for all side chain lengths, thus direct comparison with the result obtained above on the ratio of $(Q_{SS})_I$ for random ionomers and telechelics is possible. For the four series of side-chain ionomers considered in ref 37 the ratio of the values of $(Q_{SS})_I$ obtained for polymers with longest and shortest side chains is 7.77, 6.40, 4.24, and 3.74, correspondingly. Since for the polymers studied in ref 37, even for shortest side chains, the ionomeric groups were somewhat separated from the backbone (especially for the case of ether ionomers for which the values of 4.24 and 3.74 were obtained), these results are in agreement with the value 8, which is predicted above for telechelic and random ionomers.

4.2. Characteristics of Microdomain Structure. The values of intermultiplet (intermicellar) spacing for ionomers, λ, and the radius of the region where B chains are extended, D, can be obtained for this case (random ionomers in the superstrong segregation regime) as follows:

$$(\lambda_{SS})_I = \Omega\left[\frac{\gamma\pi}{6\varkappa^2}\frac{s_B}{s_A}L_B a_A^2\right]^{1/3} \tag{32}$$

$$(D_{SS})_I = \frac{\Omega^3}{6\varkappa^2}\frac{a_A^2 s_B}{l_B s_A} \tag{33}$$

By comparing three length scales, $(R_{SS})_I$ (eq 30), $(\lambda_{SS})_I$ (eq 32), and $(D_{SS})_I$ (eq 33), we conclude that for random ionomers in the superstrong segregation region the strong inequalities $R \ll D \ll \lambda$ are always valid. In general, since at $N_A = 1$ and $N_B \gg 1$ the inequality (28) is not fulfilled, the picture of possible regimes for random ionomers corresponds to Figure 6b rather than to Figure 6a. In particular, in random or telechelic ionomer melts the probability of chain return to a given micelle with the formation of a loop, β (cf. Figure 5), should be small, $\beta \ll 1$.

Another important conclusion can be drawn if one compares the value of $(\lambda_{SS})_I$ given by eq 32 with the dimension of the B chain $R_B = (L_B l_B)^{1/2}$. It turns out that for ionomers

$$(\lambda_{SS})_I \ll R_B \tag{34}$$

therefore, for large enough values of L_B, the B chains should connect relatively remote multiplets (not nearest neighbors). This fact differs from the traditional picture which has been generally assumed for the structure of random ionomers (chains connecting mainly neighbor micelles).

4.3. Strong Segregation Regime in Ionomers. Although we believe that the superstrong segregation regime is most characteristic for ionomers, the possibility of realization of a strong segregation regime at high enough temperatures

$$\frac{\delta}{kT} < \frac{\theta}{6\varkappa}\Omega^3\frac{a_A s_B}{l_B s_A^2} \tag{35}$$

should not be discarded. The main characteristics of the ionomer melt in this regime are given below (cf. eqs 14–17):

$$Q_I = \frac{\pi}{\varkappa^2}\frac{\delta}{kT}\frac{s_A a_A l_B}{s_B \theta}, \quad R_I = \left[\frac{3}{4\varkappa^2}\frac{\delta}{kT}\frac{s_A^2 a_A^2 l_B}{\theta s_B}\right]^{1/3},$$
$$\lambda_I = \left[\frac{\pi\gamma}{\varkappa}\frac{\delta}{kT}\frac{L_B l_B a_A s_A}{\theta}\right]^{1/3}, \quad D_I = \frac{1}{\varkappa}\frac{\delta}{kT}\frac{s_A a_A}{\theta} \tag{36}$$

Thus in the strong segregation regime all these characteristics depend on the temperature and parameters l_B and s_B of the B chains (cf. with eqs 29–33 describing the superstrong segregation regime).

Finally, at

$$\frac{\delta}{kT} = \left(\frac{\delta}{kT}\right)_0 \tag{37}$$

the temperature becomes so high (or, alternatively, the interdipole interaction so weak) that the equilibrium micelles are no longer formed.

4.4. Chain Extension in Ionomers. The B chains connecting multiplets in ionomer melts consist of three parts: two parts lying in the regions of high extension (within the spheres of radius D around the multiplets, cf. Figure 4) separated by a central part of the B chain exhibiting Gaussian statistics. It is clear that as a result B chains will be somewhat extended, although due to the inequalities $D \ll (\lambda_{SS})_I \ll R_B$ this extension should not be very significant. By considering different B chains as independent parts of a long ionomer macromolecule, and using the results for the extension of B chains near the multiplets (cf. the evaluation of the term F_2 above, eqs 6–8), it is easy to derive that there is some extension of ionomer chain due to its incorporation into multiplet (microdomain) structure

$$\frac{\langle S^2\rangle_I - \langle S^2\rangle_0}{\langle S^2\rangle_0} \sim \frac{D^2}{L_B l_B} \sim \frac{x^2 Q^2 {s_B}^2}{L_B {l_B}^3} \tag{38}$$

where $\langle S^2\rangle_I$ is the actual radius of gyration of the chain in the ionomer melt, while $\langle S^2\rangle_0$ is the unperturbed Gaussian radius of gyration. The value of Q in eq 38 should be determined using formula 29 or 36 in the superstrong or strong segregation regimes, correspondingly.

The expansion of ionomer chains in the melt was experimentally observed in refs 38 and 39, although this issue is still a matter of some controversy.[40] There were also theoretical attempts to describe this expansion,[41] but to the best of our knowledge the reason for the expansion which was described above (the existence of strongly expanded regions near the multiplets) has not been considered quantitatively.

4.5. Regular vs Random Ionomers. Let us now discuss possible differences in multiplet structures in ionomer melts formed by ionomer chains with ionic groups either regularly or randomly distributed along the chains.

The case of regular spacing (no polydispersity in N_B) was in fact considered above. In this case only lonely A-monomer links are present and each A link brings two B chains to emanate from the multiplet. On the other hand, for random ionomers the situations of two consecutive A links are possible (this fact was already pointed out in ref 21). These situations may not be so rare if one takes into account the correlations in the positions of A links along the chain which may appear in the course of the ionomer synthesis due to the strong interactions between A links.

From the point of view of our theory the existence of some correlation in the positions of A links leads to a significant weaking of steric restrictions: e.g. two consecutive A links give rise to only two B chains emanating from the multiplet (instead of four chains which would be the case if these two links were separated along the chain). Therefore, the size of the multiplets for this case should be larger: in our theory the number of ionomeric links in the multiplets (i.e. QN_A in our notation) is proportional to N_A^3 (eq 24); thus even a small increase in the effective value of N_A leads to a significant enlargement of multiplet size.

Therefore we conclude that at equal ionic content the multiplets for random ionomers should be larger than those for ionomers with regular spacing of ionic groups along the chain. In other words, the sequence of systems with increasing size of multiplets is as follows: ionomers with regular spacing of ionic groups, random ionomers, telechelic ionomers; i.e. random ionomers are closer to telechelics than regular ones. If there is strong cooperativity in the positions of A links in a random ionomer (effective value of $N_A > 2$), multiplets could be even larger than for telechelics.

4.6. Glass Transition in Ionomers. A major problem for the structure of ionomer melts is the existence of two glass transition temperatures.[21] This fact has led to the formulation of the concept of "clusters",[18] which are considered as rather extended regions (of size larger than 50 Å), densely cross-linked by multiplets; therefore these regions have a glass transition temperature which is different from that of the ionomer melt surrounding these regions. In the latest development of the cluster concept[21] it is assumed that clusters are percolated regions of restricted B-chain mobility. Therefore, such structural elements as clusters are of kinetic rather than thermodynamic origin and they should not appear in the pure thermodynamic consideration of the present paper.

However, we think that some of the results obtained above are relevant for the quantitative study of the structure of clusters. In particular, the regions of restricted B-chain mobility could correspond to the spheres of radius D around the multiplets where the chains are strongly extended. It is clear that strong extension corresponds to low conformational entropy and therefore to higher glass transition temperatures of these regions. From this point of view, it is more likely that the radius of the region of restricted mobility corresponds to $(D_{SS})_I$ (eq 33) rather than to l_B, as it was assumed in ref 21. However, in this case the radius of the region of restricted mobility in accordance with eq 33 should decrease with the increase of l_B, i.e. of the B-chain stiffness (roughly speaking stiff chains are "more rapidly going away" from the region of multiplet cross-links than flexible ones). This contradicts some arguments of ref 21, and this discrepancy should be resolved in the future.

On the other hand, in agreement with the point of view which was formulated in ref 21, the second glass transition temperature looks to be due to the association of the regions of restricted mobility in rather large clusters. Whether there is a thermodynamic driving force for this association is a subtle question. According to ref 21 (as well as in the framework of the model of the present paper) such a driving force is absent. However, it is not excluded that the tendency for association of multiplets can appear if one takes into account various complications of the real ionomeric systems.

For example, one of the possible explanations is the polydispersity in ionic composition between different chains. Since ionic groups are strongly interacting with each other, even a small difference between chains in the ionic content can be enough to induce a trend toward phase demixing. Indeed, for random ionomers, species with higher ionic content will have more –A–A– (or, say, –A–A–A, etc.) sequences and therefore in accordance with eqs 24 and 25 will produce larger multiplets if they are concentrated in some spatial region (cf. the discussion above). This will lower the free energy of the system; thus there should be a thermodynamic driving force for the formation of domains rich with chains (or chain parts) with higher ionic content. On the other hand, this driving force may not lead to the complete phase separation because of kinetic (high viscosity of the system) or chain connectivity (A-rich and A-poor parts belong to the same

chain) reasons. As a result, clusters of size around 100 Å may well be formed.

Clearly, the quantitative analysis of this problem requires the detailed consideration of the multiplet structure for ionomers with a correlated A–B sequence which is out of the scope of the present paper.

5. Conclusion

The aim of this paper was to demonstrate that the concepts of the theory of microphase separation in block copolymers can be fruitfully applied to the analysis of multiplet structure in ionomers. In addition to this, by studying block-copolymer systems which are most relevant from the point of view of the parallels with ionomers, we were able to describe a new superstrong segregation regime for the microdomain structure in block copolymers.

There are various ways to generalize the consideration of the present paper. First of all, it would be very interesting to study the influence of the low-molecular-weight solvent (selective or nonselective) on the microdomain structure. Second, the description of the structure for ionomers with a correlated A–B sequence will enable one to consider all the intermediate cases between random and block ionomers. Finally, the understanding of the equilibrium structure can help in studying peculiar rheological behavior of ionomers.[42-45] We are planning that these will be main directions of our further studies in this field.

Acknowledgment. This work was performed during the stay of two of the authors (A.R.K. and I.A.N.) at Nagoya University, Japan. A.R.K. would like to thank the Ministry of High Education of Japan (Monbusho) and I.A.N. is grateful to the Japanese Society for Promotion of Science who provided the opportunities for their stay in Nagoya.

Appendix 1

By substituting eq 14 into eq 12, it is possible to calculate the free energy cost for one A block, f_m, due to its incorporation into the micelle

$$f_m = kT\left[\left(\frac{\delta}{kT}\right)^2\theta\frac{L_A s_A s_B}{l_B}\right]^{1/3}\frac{3}{2}(6\varkappa)^{2/3} \qquad \text{(A1.1)}$$

On the other hand, if the A block is in the "free" state in the B-rich region its free energy, f_f, within the Flory–Huggins approximation can be written as

$$f_f = kT\chi N_A \qquad \text{(A1.2)}$$

where χ is the Flory–Huggins parameter for A–B interaction.

To compare the expressions A1.1 and A1.2, it is necessary to establish the connection between the parameters δ and χ. For simplicity let us do this for the case when all the microscopic length parameters are of the same order of magnitude ($s_A \sim s_B \sim a^2$, $l_A \sim l_B \sim a_A \sim a_B \sim a$; the consideration in the general case is much more lengthy but leads to the same results). For this case, as we are within the strong segregation regime (for $N_A \ll N_B$ only micelles with narrow interphases correspond to equilibrium[5])

$$\delta = \frac{kT}{a^2}\sqrt{\frac{\chi}{6}} \qquad \text{(A1.3)}$$

(see, for example, ref 28). Therefore, for this case we have

$$f_m/kT \sim (\chi N_A)^{1/3} \quad \text{and} \quad f_f/kT = \chi N_A \qquad \text{(A1.4)}$$

Since according to ref 5 already at the threshold of the micelle formation $\chi N_A \gg 1$, we conclude that

$$\frac{\Delta f}{kT} \equiv \frac{f_f - f_m}{kT} \gg 1 \qquad \text{(A1.5)}$$

This fact proves that the concentration of free A blocks (not incorporated into micelles) is in fact exponentially small.

Now let us consider the inequality (18) from the same point of view. In our notation, taking into account eq A1.3, it can be written as

$$\frac{\delta}{kT} \gg \frac{1}{a^2 N_A^{1/2}} \quad \text{or} \quad \chi^{1/2} \gg \frac{1}{N_A^{1/2}} \qquad \text{(A1.6)}$$

which is valid in the whole region of existence of microdomain micellar structure.

Appendix 2

To calculate the free energy, F_3, of the expansion of A chains inside the micelles, we will use the method of ref 5. The free energy F_3 is the result of minimization (with respect to $p(r_0)$ and $E(r,r_0)$) of the following functional (cf. ref 5):

$$F_3 = 2\varkappa \mathbf{N}\frac{3}{2}kT\int_0^R dr_0 \int_{r_0}^R E(r,r_0)p(r_0)\,dr\,\frac{1}{l_A a_A} \qquad \text{(A2.1)}$$

with two additional conditions

$$\int_{r_0}^R \frac{dr}{E(r,r_0)} = \frac{N_A}{2\varkappa} \qquad \text{(A2.2)}$$

$$2\varkappa Q v_A \int_0^r \frac{p(r_0)\,dr_0}{E(r,r_0)} = 4\pi r^2 \qquad \text{(A2.3)}$$

Here $p(r_0)dr_0$ is the fraction of A blocks whose middle points (in the case of polyblock copolymers, $\varkappa = 1$) or ends (for triblock copolymers, $\varkappa = 1/2$) lie at the distances between r_0 and $r_0 + dr_0$ from the center of the micelle; $E(r,r_0) = dr/dn$ is the local extension (at the distance r) of the chain with a given r_0 (cf. eqs A2.1 and 7, A2.3 and 6).

The minimization gives the result

$$F_3 = \frac{3\pi^2\varkappa^2}{20}kT\mathbf{N}\frac{R^2}{N_A a_A l_A} \qquad \text{(A2.4)}$$

which coincides with eq 9.

List of Symbols

N_A (N_B) – number of monomer links in an A block (B block)

s_A (s_B) – chain cross-section for an A (B) chain

s_{AB} – chain cross-section at an A–B junction point

l_A (l_B) – Kuhn segment length for an A (B) chain

L_A (L_B) – contour chain length of an A (B) block

$\theta \equiv 1 + (3\pi^2/40)(s_A l_B/s_B l_A)$; $\Omega \equiv \min\{1; 3s_A/s_{AB}\}$

a_A (a_B) – contour chain length per one monomer link for chains A (B), $a_\alpha = L_\alpha/N_\alpha$ (α = A, B)

v_A (v_B) – volume of a monomer link of an A (B) chain,

$\varkappa = 1$ (for polyblock copolymers) or $1/2$ (for triblock copolymers)

Q – number of A blocks in one micelle

$\mathbf{N}$ – total number of A-blocks in the system

λ – characteristic intermicellar distance

γ – structural factor which depends on the type of micellar spatial arrangement

R – radius of the micellar core filled by A blocks

D – radius of the area around the micelle where B chains are strongly extended

R_B – average end-to-end distance for a B block

β – probability of the B-block return to the same micelle with the loop formation

T – temperature

k – Boltzmann constant

δ – surface tension coefficient,

$(\delta/kT)_{cr} \equiv \varkappa\theta(L_B l_B)^{1/2}/L_A s_A$; $(\delta/kT)_{SS} \equiv (\theta/6\varkappa)(L_A s_B/l_B s_A^2)\Omega^3$

References and Notes

(1) *Processing, Structure and Properties of Block Copolymers*; Folkes, M. J., Ed.; Elsevier: New York, 1985.
(2) *Developments in Block Copolymers*; Goodman, I., Ed.; Applied Science: New York, 1982 and 1985; Vols. 1 and 2.
(3) Hadziioannou, G.; Skoulios, A. *Macromolecules* **1982**, *15*, 258.
(4) Leibler, L. *Macromolecules* **1980**, *13*, 1602.
(5) Semenov, A. N. *Sov. Phys. JETP* **1985**, *61*, 733.
(6) Dobrynin, A. V.; Erukhimovich, I. Ya. *J. Phys. II* **1991**, *1*, 1387.
(7) Benoit, H.; Hadziioannou, G. *Macromolecules* **1988**, *21*, 1449.
(8) Halperin, A. *Macromolecules* **1991**, *24*, 1418.
(9) Binder, K.; Frisch, H. *J. Chem. Phys.* **1984**, *81*, 2126.
(10) Grosberg, A. Yu.; Frisch, H. *Makromolekulare Chemie, Theory and Simulations*, to be published.
(11) Borue, V. Yu; Erukhimovich, I. Ya. *Macromolecules* **1988**, *21*, 3240.
(12) Nyrkova, I. A.; Khokhlov, A. R.; Kramarenko, E. Yu. *Polym. Sci. USSR (Engl. Transl.)* **1990**, *32*, 852. Khokhlov, A. R.; Nyrkova, I. A. *Macromolecules* **1992**, *25*, 1493.
(13) Joanny, J. F.; Leibler, L. *J. Phys.* **1990**, *51*, 545.
(14) Brereton, M. G.; Vilgis, T. A. *Macromolecules* **1990**, *23*, 2044.
(15) Shakhnovich E. I.; Gutin, A. M. *J. Phys.* **1989**, *50*, 1843.
(16) Kuchanov, S. I.; Panukov S. V. *Zh. Eksp. Teor. Fiz.* **1991**, *99*, 659.
(17) Dobrynin, A. V.; Erukhimovich, I. Ya. *JETP Lett.* **1991**, *53*, 570.
(18) Eisenberg, A. *Macromolecules* **1970**, *3*, 147.
(19) MacKnight, W. J.; Earnest T. R. *Macromol. Rev.* **1981**, *16*, 41.
(20) Mauritz, K. A. *J. Macromol. Sci., Rev. Macromol. Chem. Phys.* **1988**, *C28*, 65.
(21) Eisenberg, A.; Hird, B.; Moore, R. B. *Macromolecules* **1990**, *23*, 4098.
(22) Williams, C. E. In *Multiphase Macromolecular Systems*; Culbertson, B. M., Ed.; Plenum Press: New York, 1989; Vol. 6.
(23) Williams, C. E.; Russel, T. P.; Jerome, R.; Horrion, J. *Macromolecules* **1986**, *19*, 2877.
(24) Horrion, J.; Jerome, R.; Teyssie, Ph.; Marco, C.; Williams, C. E. *Polymer* **1988**, *29*, 1203.
(25) Gouin, J. P.; Williams, C. E.; Eisenberg, A. *Macromolecules* **1989**, *22*, 4573.
(26) Erukhimovich, I. Ya. *Vysokomolek. Soedin.* **1982**, *24A*, 1942, 1950.
(27) Fredrickson, G. H.; Helfand, E. *J. Chem. Phys.* **1987**, *87*, 697.
(28) Helfand, E.; Wasserman, Z. R. *Macromolecules* **1976**, *9*, 879; **1978**, *11*, 960; **1980**, *13*, 994.
(29) Semenov, A. N. *Macromolecules* **1989**, *22*, 2849.
(30) Dreyfus, B. *Macromolecules* **1985**, *18*, 284.
(31) Birshtein, T. M.; Zhulina, E. B. *Vysokomolek. Soedin.* **1985**, *27A*, 1613.
(32) Zhulina, E. B.; Birshtein, T. M. *Vysokomolek. Soedin.* **1987**, *29A*, 1524.
(33) Zhulina, E. B.; Semenov, A. N. *Vysokomolek. Soedin.* **1989**, *31A*, 177.
(34) De Gennes, P. G. *Scaling Concepts in Polymer Physics*; Cornell University Press: Ithaca, NY, 1979.
(35) Edwards, S. F. *Proc. R. Soc.* **1966**, *88*, 265.
(36) (a) Maybe at this point it is worthwhile to explain why we are using the term "random ionomer" in the text, although in the limit $N_A = 1$ regular polyblock copolymers which were considered in sections 2 and 3 converge to regular ionomers. In real experimental study the most common ionomeric object is a random ionomer; it is very difficult to synthesize a regular ionomer. Although there should be some delicate differences in behavior of random and regular ionomers[36b] (and we will comment on some of these issues further), these differences are in most cases less pronounced than those between random and telechelic ionomers. Therefore, in the present paper we will neglect the fact that the properties of random and regular ionomers are different (except for some comments below), and use the term random ionomer for both situations. (b) Khokhlov, A. R.; Panukov S. V. To be published.
(37) Moore, R. B.; Bittencourt, D.; Gauthier, M.; Williams, C. E.; Eisenberg, A. *Macromolecules* **1991**, *24*, 1376.
(38) Earnest, T. R.; Higgins, J. S.; Handlin, D. L.; MacKnight, W. J. *Macromolecules* **1981**, *14*, 192.
(39) Forsman, W. C.; MacKnight, W. J.; Higgins, J. S. *Macromolecules* **1984**, *17*, 490.
(40) Squires, E.; Painter, P.; Howe, S. *Macromolecules* **1987**, *20*, 1740.
(41) Forsman, W. C. *Macromolecules* **1982**, *15*, 1032.
(42) Tant, M. R.; Wilkes, G. L. *J. Macromol. Sci., Rev. Macromol. Chem. Phys.* **1988**, *C28*, 1.
(43) Witten, T. A.; Cohen, M. H. *Macromolecules* **1985**, *18*, 1915.
(44) Witten, T. A. *J. Phys.* **1988**, *49*, 1055.
(45) Ballard, M. J.; Buscal, R.; Waite, E. A. *Polymer* **1988**, *29*, 1287.